

Mechanism of the Migratory Insertion of Carbon Monoxide in the Indenyliron(II) System. Detectable Intermediates in an Associative Pathway

Donato Monti and Mauro Bassetti*

Contribution from the Centro C.N.R. di Studio sui Meccanismi di Reazione, Dipartimento di Chimica, Università "La Sapienza", 00185 Roma, Italy

Received October 12, 1992

Abstract: The indenyl complex $(\eta^5\text{-C}_9\text{H}_7)\text{Fe}(\text{CO})_2\text{Me}$ reacts with phosphines (PMe_3 , PMe_2Ph , PMePh_2 , PPh_3) in toluene to give the products of alkyl migratory insertion $(\eta^5\text{-C}_9\text{H}_7)\text{Fe}(\text{CO})(\text{phosphine})(\text{COR})$. The kinetic investigation is in agreement with a mechanism involving a rapid preequilibrium between the iron complex and the phosphine (K), followed by rate-determining alkyl migration (k_2). The reaction rates increase with decreasing cone angle and increasing basicities of the phosphines, in the order PPh_3 ($k_2K = 5.6 \times 10^{-5} \text{ M}^{-1} \text{ s}^{-1}$) < PMePh_2 ($k_2K = 7.0 \times 10^{-5} \text{ M}^{-1} \text{ s}^{-1}$) < PMe_2Ph ($k_2K = 7.4 \times 10^{-4} \text{ M}^{-1} \text{ s}^{-1}$) < PMe_3 ($9.4 \times 10^{-4} \text{ M}^{-1} \text{ s}^{-1}$), at 40.0 °C. Both the equilibrium constants for the preequilibrium step and the rate constants for C-C coupling are obtained from analysis of kinetic data. The equilibrium constant between the iron complex and PPh_3 has been measured independently by UV-visible spectroscopy. Kinetic and spectroscopic (UV-visible, IR, NMR) data are indicative of a weak interaction between the iron complex and the phosphine, in which the molecular frame of the iron complex is not perturbed.

Introduction

There is considerable interest in the enhanced reactivity of η^5 -indenyl transition-metal complexes toward ligand substitution and related reactions compared to their η^5 -cyclopentadienyl (Cp) analogues.¹ This rate enhancement is believed to be related to the greater ease of "ring slippage" from an η^5 - to an η^3 -bonding mode for the indenyl ligand.^{1,2} The hypothesis of ring slippage toward an intermediate with η^3 coordination has been supported by an interpretation of kinetic data,^{1a,c,2} by the isolation of structurally characterized η^3 -cyclopentadienyl³ and -indenyl complexes,^{3b,4} and by IR evidence from photochemically generated species.⁵ However, experimental evidence of direct nucleophile-

induced ring slippage from η^5 to η^3 ^{4d,g} and of intermediates on the reaction coordinate^{1b,6} is scarce.

There is clear evidence from kinetic experiments on molybdenum complexes that the migratory insertion of carbon monoxide into metal-alkyl bonds benefits from substitution of a cyclopentadienyl ligand by an indenyl group.⁷ The enhanced reactivity of iron indenyl complexes has been largely documented in carbonylation and related reactions.⁸ This enhanced or unique reactivity has been discussed in terms of readily accessible η^3 intermediates. The migratory insertion in indenyl iridium complexes has been recently described.⁹

With regards to reaction kinetics, available evidence for η^5 - η^3 ring slippage is based simply on second-order behavior,^{1a,c,e,7} but kinetically detectable intermediates have never been observed. In principle, means of discriminating between intermediates and transition states for ring slippage pathways are missing, and the mechanistic question is still at a speculative stage, especially regarding migratory insertion.^{8c} The matter of the reactive intermediates involved in carbonylation represents a crucial point.^{10,11}

Initial kinetic studies on the mechanism of the migratory insertion, carried out with manganese and iron alkyls, have shown that the reaction proceeds by formation of a solvent-saturated (or a coordinatively unsaturated) acyl complex, followed by attack

* Address correspondence to this author. FAX number: 39-6-490421.

(1) (a) Hart-Davis, A. J.; White, C.; Mawby, R. J. *Inorg. Chim. Acta* **1970**, *4*, 441. (b) Caddy, P.; Green, M.; O'Brien, E.; Smart, L. E.; Woodward, P. *J. Chem. Soc., Dalton Trans.* **1980**, 962. (c) Rerek, M. E.; Basolo, F. *J. Am. Chem. Soc.* **1984**, *106*, 5908. (d) Yang, G. K.; Bergman, R. G. *Organometallics* **1985**, *4*, 129. (e) Casey, C. P.; O'Connor, J. M.; Jones, W. D.; Haller, K. J. *Organometallics* **1983**, *2*, 535. (f) Casey, C. P.; O'Connor, J. M. *Organometallics* **1985**, *4*, 384. (g) Habib, A.; Tanke, R. S.; Holt, E. M.; Crabtree, R. H. *Organometallics* **1989**, *8*, 1225. (h) Kakkar, A. K.; Taylor, N. J.; Marder, T. B. *Organometallics* **1989**, *8*, 1765. (i) Bang, H.; Lynch, T. J.; Basolo, F. *Organometallics* **1992**, *11*, 40.

(2) O'Connor, J. M.; Casey, C. P. *Chem. Rev.* **1987**, *87*, 307.

(3) (a) Huttner, G.; Brintzinger, H. H.; Bell, L. G.; Friedrich, P.; Bejenke, V.; Neugebauer, D. *J. Organomet. Chem.* **1978**, *145*, 329. (b) Schonberg, P. R.; Paine, R. T.; Campana, C. F.; Duesler, E. N. *Organometallics* **1982**, *1*, 799.

(4) (a) Nesmeyanov, A. N.; Ustynyuk, N. A.; Makarova, L. G.; Andrianov, V. G.; Struchkov, Y. T.; Andrae, S.; Ustynyuk, Y. A.; Malyugina, S. G. *J. Organomet. Chem.* **1979**, *159*, 189. (b) Nakasuji, K.; Yamaguchi, M.; Murata, I.; Tatsumi, K.; Nakamura, A. *Organometallics* **1984**, *3*, 1257. (c) Faller, J. W.; Crabtree, R. H.; Habib, A. *Organometallics* **1985**, *4*, 929. (d) Merola, J. S.; Kacmarcik, R. T.; Van Engen, D. *J. Am. Chem. Soc.* **1986**, *108*, 329. (e) Kowaleski, R. M.; Rheingold, A. L.; Troglor, W. C.; Basolo, F. *J. Am. Chem. Soc.* **1986**, *108*, 2460. (f) Baker, R. T.; Tulip, T. H. *Organometallics* **1986**, *5*, 839. (g) Forschner, T. C.; Cutler, A. R.; Kullnig, R. K. *Organometallics* **1987**, *6*, 889.

(5) (a) Fettes, D. J.; Narayanaswamy, R.; Rest, A. J. *J. Chem. Soc., Dalton Trans.* **1981**, 2311. (b) Mahmoud, K. A.; Rest, A. J.; Alt, H. G. *J. Chem. Soc., Dalton Trans.* **1985**, 1365. (c) Chetwynd-Talbot, J.; Grebenik, P.; Perutz, R. N.; Powell, M. H. A. *Inorg. Chem.* **1983**, *22*, 1675. (d) Belmont, J. A.; Wrighton, M. S. *Organometallics* **1986**, *5*, 1421.

(6) Ahmed, H.; Brown, D. A.; Fitzpatrick, N. J.; Glass, W. K. *J. Organomet. Chem.* **1991**, *418*, C14.

(7) Hart-Davis, A. J.; Mawby, R. J. *J. Chem. Soc. A* **1969**, 2403.

(8) (a) Forschner, T. C.; Cutler, A. R. *Organometallics* **1985**, *4*, 1247. (b) Levitre, S. A.; Cutler, A. R.; Forschner, T. C. *Organometallics* **1989**, *8*, 1133. (c) Forschner, T. C.; Cutler, A. R.; Kullnig, R. K. *J. Organomet. Chem.* **1988**, *356*, C12. (d) Forschner, T. C.; Cutler, A. R. *J. Organomet. Chem.* **1989**, *361*, C41.

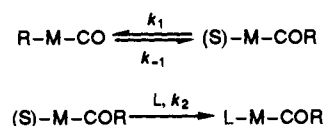
(9) Foo, T.; Bergman, R. G. *Organometallics* **1992**, *11*, 1811.

(10) Collman, J. A.; Hegedus, L. S.; Norton, J. R.; Finke, R. G. *Principles and Applications of Organotransition Metal Chemistry*; University Science Books: Mill Valley, CA, 1987.

(11) (a) Nicholas, K.; Raghu, S.; Rosenblum, M. *J. Organomet. Chem.* **1974**, *78*, 133. (b) Jablonski, C. R.; Wang, Y. P. *Inorg. Chim. Acta* **1983**, *69*, 171. (c) Jablonski, C.; Bellachioma, G.; Cardaci, G.; Reichenbach, G. *J. Am. Chem. Soc.* **1990**, *112*, 1632. (d) Haynes, A.; Mann, B. E.; Gulliver, D. J.; Morris, G. E.; Maitlis, P. M. *J. Am. Chem. Soc.* **1991**, *113*, 8567.

of the incoming ligand to give the final acyl product.¹² This is described in Scheme I (S = solvent),

Scheme I



and by eq 1

$$k_{\text{obs}} = \frac{k_1 k_2 [\text{L}]}{k_{-1} + k_2 [\text{L}]} \quad (1)$$

This mechanism, which is generally accepted for reactions involving coordinatively saturated 18-electron alkylmetal carbonyls,¹⁰ does not involve participation of the reacting ligand L in the acyl-forming step (k_1). On the other hand, the role of nucleophiles has often been pointed out and evidence has been presented that the reaction is assisted by incorporation of a nucleophile solute or solvent.^{13,14} Our recent studies on the reaction of Rh(III) methyl and phenyl carbonyl complexes with triphenylphosphine in toluene have indicated that the phosphine is part of the rate-limiting step,¹⁵ except when an appropriate carboxylate ligand acts as an internal nucleophile.^{15c}

It is well known that alkyl-to-acyl migratory insertions are enormously accelerated in odd-electron organometallic complexes, either 17- or 19-electron species.¹⁶ However, there is controversy over whether the insertion step occurs before or after coordination of the incoming nucleophile, and there seems to be no consensus of opinion on the reaction mechanism.^{16a,17} Recently, evidence has been presented that the carbonylation of $(\eta^5\text{-C}_5\text{H}_5\text{-L})(\text{CO})\text{FeMe}^+$ is nucleophilically assisted.^{16e,17c}

We now report a kinetic investigation of the migratory insertion of carbon monoxide for the iron(II) indenyl complex $(\eta^5\text{-C}_9\text{H}_7)\text{Fe}(\text{CO})_2(\text{Me})$. This paper presents clean evidence of an associative pathway for the migratory insertion in an iron(II) 18-electron complex and the first kinetic and spectroscopic evidence of molecular association between an indenyl complex and a reacting phosphine.

Experimental Section

General Data. ¹H NMR spectra were recorded on a Bruker WP-80 spectrometer and ¹³C spectra on a Varian XL-300 spectrometer. Chemical shifts (ppm) are relative to tetramethylsilane. ³¹P{¹H} NMR spectra were obtained on a Bruker AM-300 instrument. IR spectra were measured with a Nicolet 510 FT-IR spectrometer interfaced to a Nicolet 620 workstation, using 0.1-mm CaF₂ cells. UV-visible and kinetic mea-

surements were obtained with Varian Cary 219 and Cary 1 spectrophotometers. Elemental analyses were performed by the Servizio di Microanalisi at the Area della Ricerca (C.N.R., Monterotondo Stazione). Mass spectra were obtained on a VG Quattro triple quadrupole spectrometer at the Università di Roma "Tor Vergata".

Unless otherwise indicated, all reactions were carried out under nitrogen or argon using standard Schlenk-line techniques. Toluene was distilled under nitrogen from sodium benzophenone. Hexane was distilled from sodium. Alumina (3% water) was used for chromatography. Chemicals and solvents were reagent grade. The phosphines were obtained from commercial sources (Aldrich) and used as received. Triphenylphosphine was recrystallized from ethanol. $[(\text{C}_5\text{H}_5)\text{Fe}(\text{CO})_2]_2$ was commercially available; $[(\text{C}_9\text{H}_7)\text{Fe}(\text{CO})_2]_2$, $(\text{C}_9\text{H}_7)\text{Fe}(\text{CO})_2\text{Me}$ (**1**)¹⁸ and $(\text{C}_5\text{H}_5)\text{Fe}(\text{CO})_2\text{Me}$ ¹⁹ were prepared as described in the literature. The methyl complex **1** decomposes slowly both in the solid state and in solution; it was stored in a freezer and purified by column chromatography, using hexane as eluant, before use.

Product analyses of the acyl complexes **2a-c** and **2d**^{8a} were carried out in toluene with the phosphine in about 10% excess and by following the reaction by infrared until completion. The complexes were generally purified by column chromatography by elution with THF and obtained in yields of about 70%. ¹H and ¹³C NMR (CDCl₃) spectra and analytical data of the complexes are as follows.

$(\text{C}_9\text{H}_7)\text{Fe}(\text{CO})(\text{PMe}_3)(\text{COMe})$ (**2a**). Oil. ¹H NMR: δ 7.5–6.9 (AA'BB', 4 H, benzo), 5.19, 5.01, 4.76 (3 br s, 3 H, C₂H, C_{1,3}H), 2.46 (s, 3 H, COMe), 1.05 (d, 9 H, $J_{\text{PH}} = 8.8$ Hz, PMe₃). ¹³C NMR: δ 276.6 (complex d, $J_{\text{PC}} = 21$ Hz, COMe), 218.97 (d, $J_{\text{PC}} = 27.7$ Hz, CO), 125.87 (C_{5,6}), 123.87 and 122.15 (C_{4,7}), 108.68 and 103.45 (C_{3a,7a}), 97.54, 73.15, and 67.75 (C_{1,2,3}), 50.60 (d, $J_{\text{PC}} = 4.5$ Hz, COMe), 16.32 (d, $J_{\text{PC}} = 28.7$ Hz, PMe₃). MS (EI): m/e (relative intensity) 318.0 (16, P⁺), 290.0 (21, [P – CO]⁺), 246.9 (base, [P – COCOMe]⁺), 170.8 (66, C₉H₇Fe⁺).

$(\text{C}_9\text{H}_7)\text{Fe}(\text{CO})(\text{PMe}_2\text{Ph})(\text{COMe})$ (**2b**). Oil. ¹H NMR: δ 7.5–6.5 (m, benzo and PPh), 5.27 (s, 1 H, C₂H), 4.85–4.70 (m, 2 H, C_{1,3}H), 2.43 (s, 3 H, COMe), 1.62 (d, $J_{\text{PH}} = 9.5$ Hz, 3 H, PMe), 1.13 (d, $J_{\text{PH}} = 9.0$ Hz, 3 H, PMe). ¹³C NMR: δ 275.8 (COMe), 220.8 (CO), 135.8 (d, $J_{\text{PC}} = 34.1$ Hz, PPh C_{ipso}), 131.2 (d, 7.6 Hz, PPh), 128.0 (d, 8.3 Hz, PPh), 124.7 (d, 11.3 Hz, PPh), 129.05 (C_{5,6}), 125.55 and 122.44 (C_{4,7}), 108.08 and 104.76 (C_{3a,7a}), 98.82, 75.15, and 66.28 (C_{1,2,3}), 50.6 (d, $J_{\text{PC}} = 6.0$ Hz, COMe), 19.8 (d, $J_{\text{PC}} = 24.9$ Hz, PMe), 17.2 (d, $J_{\text{PC}} = 27.9$ Hz, PMe). MS (EI): m/e (relative intensity) 380.4 (30, P⁺), 352.7 (92, [P – CHO]⁺), 170.8 (63, C₉H₇Fe⁺), 114.8 (base, C₉H₇⁺).

$(\text{C}_9\text{H}_7)\text{Fe}(\text{CO})(\text{PMePh}_2)(\text{COMe})$ (**2c**). Mp: 136–138 °C. ¹H NMR: δ 7.5–6.5 (m, benzo and PPh₂), 5.16 (tr, $J_{\text{HH}} = 4.5$ Hz, 1 H, C₂H), 4.91–4.85 (m, 2 H, C_{1,3}H), 2.08 (d, $J_{\text{PH}} = 0.6$ Hz, 3 H, COMe), 1.94 (d, $J_{\text{PH}} = 8.9$ Hz, 3 H, PMe). ¹³C NMR: δ 275.40 (d, $J_{\text{PC}} = 24.0$ Hz, COMe), 220.09 (d, $J_{\text{PC}} = 24.9$ Hz, CO), 136.4 (d, $J_{\text{PC}} = 44.9$ Hz, PPh₂ C_{ipso}), 135.06 (d, $J_{\text{PC}} = 40.7$ Hz, PPh₂ C_{ipso}), 131.77, 131.63, 131.55, 131.43, 129.38, 129.1, 127.96, 127.84, 127.74, and 124.96 (Ph₂), 126.41–122.08 (C_{4,5,6,7}), 109.34 and 103.82 (C_{3a,7a}), 99.19, 75.21, and 67.25 (C_{1,2,3}), 50.1 (d, $J_{\text{PC}} = 6.2$ Hz, COMe), 14.3 (d, $J_{\text{PC}} = 27.7$ Hz, PMe). Anal. Calcd for C₂₅H₂₃FeO₂P: C, 67.89; H, 5.24. Found: C, 67.37; H, 5.11.

Kinetic and Spectroscopic Studies. Kinetic experiments were carried out under pseudo-first-order conditions, using a large excess of phosphine, by UV-visible spectroscopy. Solutions of triphenylphosphine were mixed under argon with solutions of the complex, made up anaerobically in toluene, in 1-cm quartz cells. The other phosphines were added as neat liquids, or as a 1.0 M solution in the case of PMe₃, through a hypodermic syringe to solutions of the complex in the cell under an argon atmosphere. The cells were sealed tightly with a Teflon-brand stopper, shaken, and placed in the thermostated cell holder. Five kinetic runs were performed simultaneously in the instrument. The increase in absorbance associated with product formation was followed with time. Plots of $-\ln(A_\infty - A_t)$ vs time were linear over four half-lives, and pseudo-first-order rate constants (k_{obs}) were determined from the slope of this line by the least-squares method. Optimized values of k_{obs} were obtained by fitting the exponential dependence of the absorbance vs time data by using a nonlinear least-squares regression program, which provides values of k_{obs} and A_∞ . Values of A_∞ were generally well-defined and were determined by the Mangelsdorf's method in the case of the slowest reactions.²⁰ Fittings of k_{obs} to eq 3, to give the parameters k_2 and K , and of ΔA to eq 5 (equations

(12) (a) Mawby, R. J.; Basolo, F.; Pearson, R. G. *J. Am. Chem. Soc.* **1964**, *86*, 3994. (b) Butler, I. S.; Basolo, F.; Pearson, R. G. *Inorg. Chem.* **1967**, *6*, 2074.

(13) Webb, S. L.; Giandomenico, C. M.; Halpern, J. *J. Am. Chem. Soc.* **1986**, *108*, 345.

(14) (a) Wax, M. J.; Bergmann, R. G. *J. Am. Chem. Soc.* **1981**, *103*, 7028. (b) Axe, F. U.; Marynick, D. S. *Organometallics* **1987**, *6*, 572. (c) Martin, B. D.; Warner, K. E.; Norton, J. R. *J. Am. Chem. Soc.* **1986**, *108*, 33.

(15) (a) Bassetti, M.; Sunley, G. J.; Maitlis, P. M. *J. Chem. Soc., Chem. Commun.* **1988**, 1012. (b) Bassetti, M.; Sunley, G. J.; Fanizzi, F. P.; Maitlis, P. M. *J. Chem. Soc., Dalton Trans.* **1990**, 1799. (c) Monti, D.; Bassetti, M.; Sunley, G. J.; Ellis, P.; Maitlis, P. M. *Organometallics* **1991**, *10*, 4015.

(16) (a) Magnuson, R. H.; Meirowitz, R.; Zulu, S.; Giering, W. P. *J. Am. Chem. Soc.* **1982**, *104*, 5791. (b) Golovin, M. N.; Meirowitz, R.; Rahman, M. M.; Liu, H.-Y.; Prock, A.; Giering, W. P. *Organometallics* **1987**, *6*, 2285. (c) Sheridan, J. B.; Han, S.-H.; Geoffroy, G. L. *J. Am. Chem. Soc.* **1987**, *109*, 8097. (d) Gipson, S. L.; Kneten, K. *Inorg. Chim. Acta* **1989**, *157*, 143. (e) Prock, A.; Giering, W. P.; Greene, J. E.; Meirowitz, R. E.; Hoffman, S. L.; Woska, D. C.; Wilson, M.; Chang, R.; Chen, J.; Magnuson, R. H.; Eriks, K. *Organometallics* **1991**, *10*, 3479.

(17) (a) Doxsee, K. M.; Grubbs, R. H.; Anson, F. C. *J. Am. Chem. Soc.* **1984**, *106*, 7819. (b) Reger, D. L.; Mintz, E.; Lebiada, L. *J. Am. Chem. Soc.* **1986**, *108*, 1940. (c) Therien, M. J.; Troglor, W. C. *J. Am. Chem. Soc.* **1987**, *109*, 5127. (d) Liu, H.-Y.; Golovin, M. N.; Fertal, D. A.; Tracey, A. A.; Eriks, K.; Giering, W. P.; Prock, A. *Organometallics* **1989**, *8*, 1454. (e) Donovan, B. T.; Geiger, W. E. *Organometallics* **1990**, *9*, 865.

(18) Forschner, T. C.; Cutler, A. R. *Inorg. Chim. Acta* **1985**, *102*, 113.

(19) Ellis, J. E.; Flom, E. A. *J. Organomet. Chem.* **1975**, *99*, 263.

(20) Mangelsdorf, P. C. *J. Appl. Phys.* **1959**, *30*, 442.

Table I. Carbonyl Stretching Frequencies (± 0.2 cm^{-1} , hexane) for $(\eta^5\text{-C}_9\text{H}_7)\text{Fe}(\text{CO})_2\text{Me}$ and $(\eta^5\text{-C}_9\text{H}_7)\text{Fe}(\text{COMe})(\text{CO})(\text{phosphine})$ Complexes

complex	phosphine	ν_{CO}	ν_{COR}^a
1		2011.7 1957.9	
2a	PMe_3	1920.2	1626
2b	PMe_2Ph	1920.5	1616
2c	PMePh_2	1923.7	1617
2d	PPh_3	1924.2	1632

^a Broad.

in Results section), to give K and $\Delta\epsilon$, were obtained with nonlinear least-squares calculations, carried out by the program Kaleidagraph.

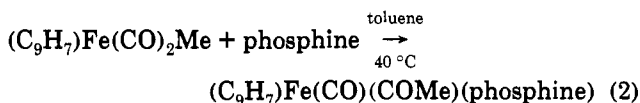
Duplications of single kinetic runs were reproducible to within 5%, and the parameters K and k_2 were reproducible to within 15% on duplication of a full kinetic set. Activation parameters for the reaction with PPh_3 were obtained by a linear least-squares analysis of the dependence of $\ln(k_2/T)$ on $1/T$. Blank experiments on solutions of the iron complex (10^{-4} M) in the absence of phosphine showed no significant decomposition during the time required for the kinetic runs both in the dark and under irradiation at 400 nm.

The study of the spectral changes associated with the interaction between complex **1** and PPh_3 was performed using a Varian Cary 210 spectrophotometer, an instrument of high quality optics and high stability (0.0004 A/hr at constant temperature). Aliquots (1 mL) of the complex and phosphine solutions were added into the separate cell compartments of a tandem-mix quartz cell (2×0.437 cm). The cell was sealed with a Teflon-brand stopper, time was allowed for thermal equilibration, and a spectrum was recorded between 460 and 340 nm. The cell was removed from the cell holder, shaken vigorously to ensure mixing of the two solutions, and immediately replaced in the spectrophotometer to obtain a new spectrum in the overlay mode. A digital readout at different wavelengths during scanning was simultaneously recorded by a printer. Further scanning of the solution gave spectra which were superimposable with regard to that obtained after mixing. The spectra, obtained in the double beam mode, were recorded before and after mixing for each phosphine solution. The reference solution, in a matched tandem-mix quartz cell, contained 1 mL of toluene and 1 mL of the same triphenylphosphine concentration as the sample solution for each of the coupled spectra, in order to ensure the same refractive index in the reference and in the sample.

Kinetic experiments were also carried out by IR spectroscopy in a thermostated 0.5-mm CaF_2 cell by monitoring the disappearance of the carbonyl stretching band at higher frequency (2004 cm^{-1}) of the starting complex and the appearance of the carbonyl band of the product, obtaining the same value of k_{obs} ; the carbonyl band of **1** at 1947 cm^{-1} is disturbed by strong solvent absorption. This method yielded half-life times within 10% of those obtained by the UV-visible experiments.

Results

Reaction and Kinetics. The complex $(\eta^5\text{-C}_9\text{H}_7)\text{Fe}(\text{CO})_2\text{Me}$ (**1**) reacted with PMe_3 , PMe_2Ph , PMePh_2 , and PPh_3 in toluene to give the corresponding acyl complexes $(\eta^5\text{-C}_9\text{H}_7)\text{Fe}(\text{CO})(\text{COMe})(\text{phosphine})$ (**2a-d**) as the unique reaction products (eq 2).



Infrared data for alkyl and acyl complexes are reported in Table I. The reactions were spectroscopically quantitative, as determined by IR and ^1H NMR.

Our study was carried out in toluene in order to minimize effects from nucleophilic assistance by the solvent and from reaction pathways where the formation of solvent-coordinated intermediates would be dominant. The kinetics of reaction 2 were carried out under pseudo-first-order conditions using a large excess (>10-fold) of phosphine. The reaction was followed at 40.0 $^\circ\text{C}$ by monitoring the increase in absorbance at ca. 400 nm

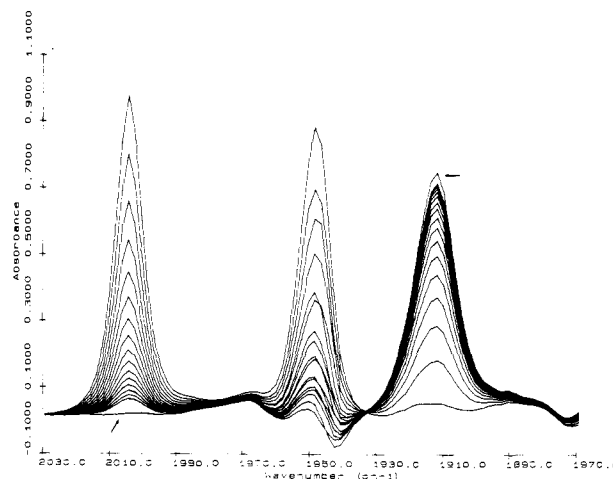


Figure 1. FTIR spectral changes during the reaction of $(\text{C}_9\text{H}_7)\text{Fe}(\text{CO})_2\text{Me}$ (7.7×10^{-3} M) with PMe_2Ph (0.489 M) to yield $(\text{C}_9\text{H}_7)\text{Fe}(\text{COMe})(\text{CO})(\text{PMe}_2\text{Ph})$, in toluene at 40 $^\circ\text{C}$ ($\rightarrow = t_\infty$). Spectra subtracted from toluene.

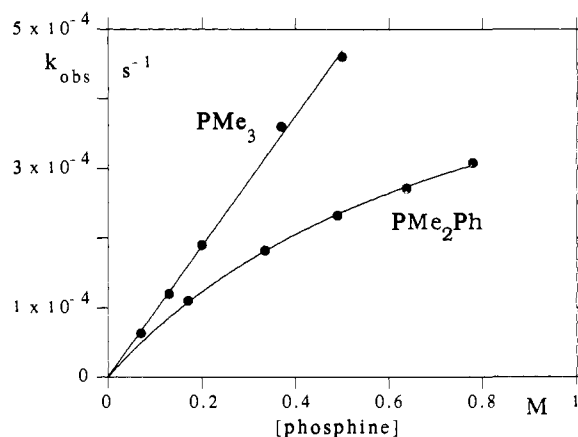


Figure 2. Plot of k_{obs} vs phosphine concentration for the reactions of $(\text{C}_9\text{H}_7)\text{Fe}(\text{CO})_2\text{Me}$ with PMe_3 and PMe_2Ph , in toluene at 40.0 $^\circ\text{C}$.

due to product formation in the visible region and the disappearance of the ν_{CO} bands of the iron complex in the infrared. The changes in the carbonyl region of the infrared are shown in Figure 1. The iron complex **1** has a broad absorption band in the visible region ($\lambda_{\text{max}} = 400$ nm, $\epsilon = 830 \pm 10$ $\text{M}^{-1} \text{cm}^{-1}$), and the products $(\text{C}_9\text{H}_7)\text{Fe}(\text{CO})(\text{COMe})(\text{phosphine})$ have absorption spectra similar to those of the parent compound, with an increase in intensity (λ_{max} of **2c** = 382 nm, $\epsilon = 3800$ $\text{M}^{-1} \text{cm}^{-1}$). The kinetics of the reaction with PPh_3 were also studied at 50 and 60 $^\circ\text{C}$; the reaction was affected by substantial decomposition of the substrate at higher temperatures, and it was too slow at temperatures less than 40 $^\circ\text{C}$. First-order rate constants obtained by monitoring the same reaction by UV-visible and FTIR spectroscopy were in good agreement.

The reactions were first order in the methyl complex $(\text{C}_9\text{H}_7)\text{Fe}(\text{CO})_2\text{Me}$. The dependence of the rate of reaction 2 on the concentration of phosphine is shown in Figure 2 for PMe_3 and PMe_2Ph and in Figure 3 for PMePh_2 and PPh_3 . The observed rate constants, k_{obs} , are reported in Table II. Reaction 2 is not first order with respect to the P-donor nucleophiles. The observed pseudo-first-order rate constants, k_{obs} , follow a nonlinear dependence on the concentration of the phosphines, except for PMe_3 . With increasing concentration of the nucleophile, the reactivity tends toward a limiting value (*saturation kinetics*). This can be accounted for by either the mechanism in Scheme I or by some sort of complex formation of the reactants, followed by rate-

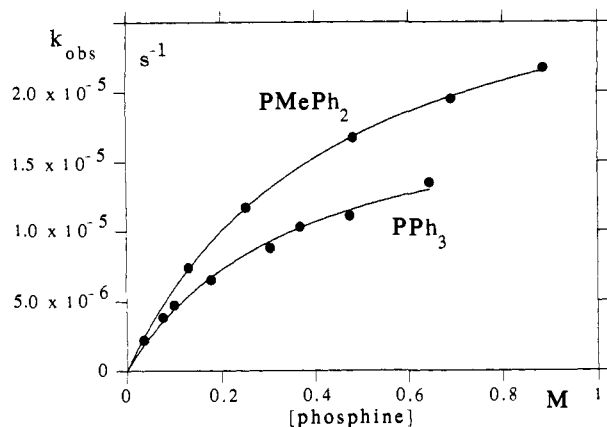


Figure 3. Plot of k_{obs} vs phosphine concentration for the reactions of $(\text{C}_9\text{H}_7)\text{Fe}(\text{CO})_2\text{Me}$ with PMePh_2 and PPh_3 , in toluene at $40.0\text{ }^\circ\text{C}$.

Table II. Observed Rate Constants, k_{obs} , for the Reaction of $(\text{C}_9\text{H}_7)\text{Fe}(\text{CO})_2\text{Me}$ (1) with PMe_3 , PMe_2Ph , PMePh_2 , and PPh_3 in Toluene at $40.0\text{ }^\circ\text{C}$

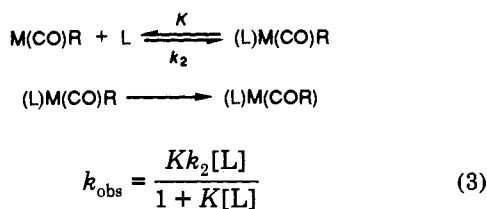
trimethylphosphine ^a		dimethylphenylphosphine ^b		methylphenylphosphine ^b	
[PMe_3], M	k_{obs} , s ⁻¹	[PMe_2Ph], M	k_{obs} , s ⁻¹	[PMePh_2], M	k_{obs} , s ⁻¹
0.50	4.6×10^{-4}	0.781	3.08×10^{-4}	0.886	2.17×10^{-5}
0.37	3.6×10^{-4}	0.639	2.71×10^{-4}	0.693	1.95×10^{-5}
0.20	1.9×10^{-4}	0.490	2.32×10^{-4}	0.483	1.67×10^{-5}
0.13	1.2×10^{-4}	0.335	1.82×10^{-4}	0.253	1.17×10^{-5}
0.07	6.3×10^{-5}	0.171	1.10×10^{-4}	0.130	7.39×10^{-6}

triphenylphosphine ^a		triphenylphosphine ^c		triphenylphosphine ^d	
[PPh_3]	k_{obs} , s ⁻¹	[PPh_3]	k_{obs} , s ⁻¹	[PPh_3]	k_{obs} , s ⁻¹
0.646	1.35×10^{-5}	0.496	3.53×10^{-5}	0.422	7.21×10^{-5}
0.475	1.11×10^{-5}	0.320	3.13×10^{-5}	0.332	6.25×10^{-5}
0.368	1.03×10^{-5}	0.269	2.81×10^{-5}	0.248	5.59×10^{-5}
0.304	8.80×10^{-6}	0.204	2.17×10^{-5}	0.0821	2.54×10^{-5}
0.178	6.52×10^{-6}	0.0969	1.48×10^{-5}		
0.100	4.71×10^{-6}				
0.0762	3.83×10^{-6}				
0.0357	2.18×10^{-6}				

^a $\lambda = 400\text{ nm}$. ^b $\lambda = 380\text{ nm}$. ^c $t = 50.0\text{ }^\circ\text{C}$. ^d $t = 60.0\text{ }^\circ\text{C}$.

determining breakdown of the new species.²¹ The latter case is described in Scheme II and by eq 3 ($L = \text{phosphine}$),²² which has the same form as the Michaelis–Menten equation.

Scheme II



The curved plots shown in Figures 2 and 3 are described correctly by either eq 1 or 3. However, the reactivity at infinite concentration of phosphine represents k_1 for the mechanism in Scheme I or k_2 for the mechanism in Scheme II. A dependence on the nature of the phosphine would be expected for the rate constant k_2 of the alkyl migration step from the intermediate species $(\text{L})\text{M}(\text{CO})\text{R}$ (Scheme II). Figures 2 and 3 show that reactivity reaches different limiting values for all phosphines. The reaction rates at infinite concentration are therefore related

(21) Jenks, W. P. *Catalysis in Chemistry and Enzymology*; McGraw-Hill, Inc.: New York, 1969; p 572.

(22) In eq 3, it is assumed that the rate is equal to the breakdown of the intermediate $(\text{L})\text{M}(\text{CO})\text{R}$ and the conservation equation is used for the total added $\text{M}(\text{CO})\text{R}$ complex.

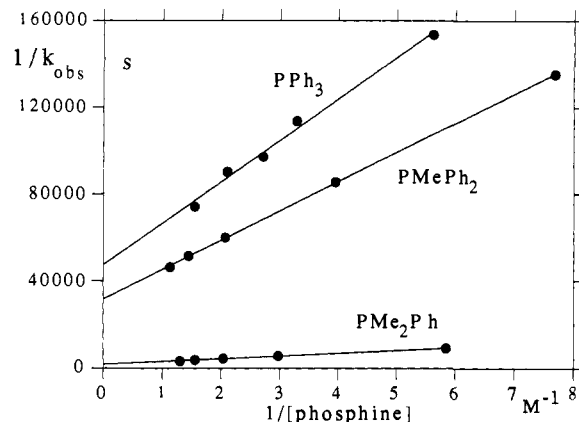


Figure 4. Plot of $1/k_{\text{obs}}$ vs $1/[\text{phosphine}]$ for the reactions of $(\text{C}_9\text{H}_7)\text{Fe}(\text{CO})_2\text{Me}$.

Table III. Kinetic Parameters for the Reaction of Complex $(\text{C}_9\text{H}_7)\text{Fe}(\text{CO})_2\text{Me}$ (1) with Phosphines, in Toluene at $40.0\text{ }^\circ\text{C}$

phosphine	K , M ⁻¹	k_2 , s ⁻¹	k_2K , M ⁻¹ s ⁻¹	$\text{p}K_a$	θ , deg
PMe_3			9.4×10^{-4}	8.65	118
PMe_2Ph	1.2 ± 0.1	$(6.2 \pm 0.3) \times 10^{-4}$	7.4×10^{-4}	6.5	122
PMePh_2	2.2 ± 0.1	$(3.2 \pm 0.1) \times 10^{-5}$	7.0×10^{-5}	4.57	136
PPh_3	2.8 ± 0.4	$(2.0 \pm 0.2) \times 10^{-5}$	5.6×10^{-5}	2.73	145
	3.5 ± 0.8^a	$(5.7 \pm 0.6) \times 10^{-5}^a$	2.0×10^{-4}		
	3.1 ± 0.5^b	$(1.3 \pm 0.1) \times 10^{-4}^b$	4.0×10^{-4}		

^a $t = 50.0\text{ }^\circ\text{C}$. ^b $t = 60.0\text{ }^\circ\text{C}$.

to the type of phosphine, thus ruling out the possibility of the mechanism in Scheme I, in which the rate constant $k_{\text{obs}} = k_1$ must be independent of the nucleophile. The experiments are in agreement with the associative mechanism described in Scheme II and by eq 3. This requires that plots of the reciprocal of the observed rate constants vs the reciprocal of nucleophile (L) concentrations are linear with a positive intercept, according to eq 4.

$$\frac{1}{k_{\text{obs}}} = \frac{1}{k_2K[\text{L}]} + \frac{1}{k_2} \quad (4)$$

A plot of $1/k_{\text{obs}}$ vs $1/[L]$ for the reactions of complex 1 with PMe_2Ph , PMePh_2 , and PPh_3 is shown in Figure 4, where the reciprocals of the y intercept represent the reactivity at infinite concentration of nucleophile.

Initial values of the K and k_2 parameters, obtained from the double reciprocal (Lineweaver–Burk) plots, were further refined by a nonlinear least-squares procedure to give the best fit to eq 3. The close adherence of the data to eq 3 is graphically shown in Figures 2 and 3 by the good fit of the experimental points to the calculated curves. The optimized parameters K and k_2 for the reactions of the complex $(\text{C}_9\text{H}_7)\text{Fe}(\text{CO})_2\text{Me}$ with different phosphines are reported in Table III, together with their standard deviations and the products k_2K , which represent the reactivity in the range of concentration used. The reaction of complex 1 with PMe_3 follows a linear dependence on phosphine concentration (Figure 2). This is still in agreement with the mechanism of Scheme II, under the condition that $1 > K[\text{L}]$, which gives $k_{\text{obs}} = Kk_2[\text{L}]$.

The reactions of the cyclopentadienyl methyl complex $(\text{C}_5\text{H}_5)\text{Fe}(\text{CO})_2\text{Me}$ with PMePh_2 and PMe_2Ph , although following the course of eq 2, were very sluggish and showed a complicated kinetic behavior.

Spectroscopic Studies. The spectra of complex 1 and PPh_3 , separately introduced in a quartz cell with an internal septum, were recorded in the UV–visible region before and immediately after the mixing of the two solutions. The experiments were carried out at temperatures ($13\text{--}16\text{ }^\circ\text{C}$) lower than that used in

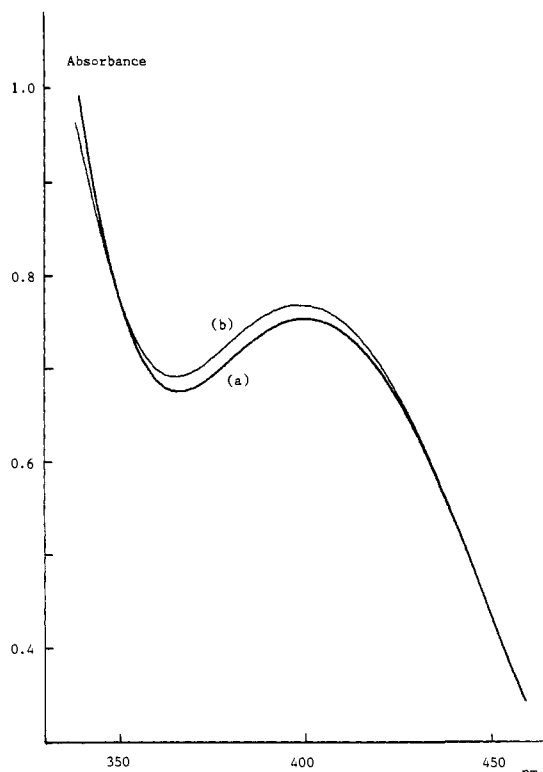


Figure 5. UV-visible spectra of $(C_9H_7)Fe(CO)_2Me$ (1 mL, 2.1×10^{-3} M) before (a) and immediately after (b) mixing with PPh_3 (1 mL, 0.70 M) in a tandem-mix quartz cell ($l = 0.874$ cm), in toluene at 15.9 °C.

Table IV. Changes of Absorbance (ΔA)^a of $(C_9H_7)Fe(CO)_2Me$ in the UV-Vis Region, Before and After Rapid Mixing with Solutions of PPh_3 , in Toluene

ΔA , 400 nm ^{b,c}	ΔA , 375 nm ^{b,d}	$[PPh_3]$	ΔA , 400 nm ^e	$[PPh_3]$
0.0039	0.0034	0.0457	0.0194	0.0378
0.0063	0.0051	0.127	0.0350	0.133
0.0112	0.0111	0.234	0.0376	0.244
0.0172	0.0175	0.349	0.0480	0.335
0.0151	0.0174	0.513	0.0599	0.508
0.0183	0.020	0.717	0.0664	0.684

^a $l = 0.874$ cm. ^b $[1] = 1.05 \times 10^{-3}$ M, $t = 15.9$ °C. ^c $A = 0.755$. ^d $A = 0.685$. ^e $[1] = 3.1 \times 10^{-3}$ M, $A = 2.250$, $t = 13.5$ °C.

the kinetic experiments in order to minimize both the formation of the product and any effect from the slow decomposition of the iron complex in solution. The mixing produces a sudden increase in absorbance of the broad band of complex **1** (Figure 5). An effect due to a change in the nature of solvent can be safely excluded, since it is already observed at concentrations of phosphine as low as 0.05 M and the increase is a function of the iron complex concentration. Although the formation of the product is also characterized by an increase in absorbance in the same region, the progress of the reaction toward the formation of $(C_9H_7)Fe(CO)(COMe)(PPh_3)$ can be excluded at this stage. In fact, further scanning of the spectrum produces a pattern identical to that obtained after mixing, showing that the reaction at this temperature does not proceed at an observable extent. The increase in absorbance is a nonlinear function of the concentration of triphenylphosphine. Values of ΔA , at two wavelengths and two different concentrations of **1**, vs PPh_3 are reported in Table IV and shown graphically in Figure 6. The trend is similar to that observed in the kinetic experiments, the jump in absorbance (ΔA) tending toward a limiting value. These experiments represent spectroscopic evidence of the first stage in Scheme II. The UV-visible pattern observed after mixing is the sum of the spectrum of the iron complex **1** and that of a species of molecular formula $[(C_9H_7)Fe(CO)_2Me-PPh_3]$.

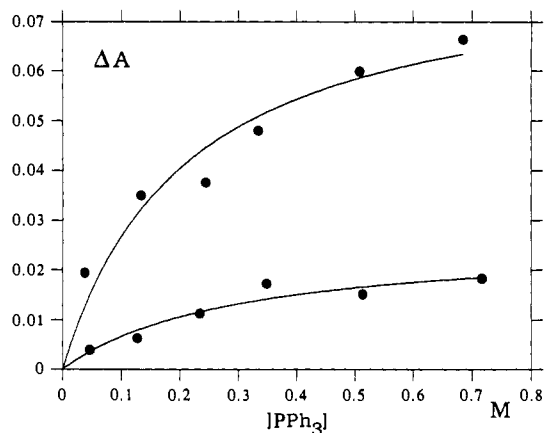


Figure 6. Changes of absorbance at $\lambda = 400$ nm upon mixing of $(C_9H_7)Fe(CO)_2Me$ with PPh_3 vs phosphine concentration. Upper curve, $[1] = 3.1 \times 10^{-3}$ M; lower curve, $[1] = 1.05 \times 10^{-3}$ M.

A nonlinear least-squares analysis of the dependence of ΔA on $[PPh_3]$ to give the best fit to eq 5 yields a value of equilibrium constant $K = 3.4 \pm 1.6$ M⁻¹ at 15.9 °C. Equation 5 is the binding

$$\Delta A = \frac{(b\Delta\epsilon S_t)K[PPh_3]}{1 + K[PPh_3]} \quad (5)$$

ΔA = change in absorbance at the same wavelength

b = optical path length (0.874 cm)

S_t = total initial concentration of $(C_9H_7)Fe(CO)_2Me$

$\Delta\epsilon$ = difference in molar absorptivity between $(C_9H_7)Fe(CO)_2Me$ and $[(C_9H_7)Fe(CO)_2Me-PPh_3]$

isotherm for the formation of a 1:1 complex.²³ In consideration of the invariance of K with temperature, as indicated by the kinetic experiments, and of the small spectral changes associated with the formation of the new species, the value of the equilibrium constant found by the spectrophotometric measurements is in satisfactory agreement with the values obtained by the kinetic method. An error due to a change in the medium upon mixing of the iron complex and of the phosphine solution can be excluded, since apparent association constants arising from medium effects are on the order of ≤ 0.2 M⁻¹,²⁴ which is the lowest limit of the stability constants which can be obtained spectrophotometrically.

The difference in molar absorptivity between complex **1** and the species $[(C_9H_7)Fe(CO)_2Me-PPh_3]$ is optimized by the computational method to the value $\Delta\epsilon = 28 \pm 6$ M⁻¹ cm⁻¹.

The ¹H NMR and FTIR bands of $(C_9H_7)Fe(CO)_2Me$ do not show changes indicative of structural variations while reacting with the phosphines with respect to the spectra of the complex alone. The carbonyl stretching bands of complex **1**, at 2004.2 and 1947.6 cm⁻¹ in toluene, are shifted to 2003.6 and 1946.8 cm⁻¹, respectively, in a 0.89 M solution of triphenylphosphine at room temperature. In the ¹H NMR spectrum, the doublet of the $C_{1,3}H$ protons (δ 4.63, $J = 2.8$ Hz) and the triplet of the C_2H proton (δ 4.15, $J = 2.8$ Hz) of **1** are shifted downfield by 1.7 and 1.5 (± 0.2) Hz, respectively, in toluene-*d*₈ at 0 °C in a solution of triphenylphosphine (0.39 M). Line broadening is not observed in the presence of PPh_3 , presumably due to rapid exchange within the molecular complex. The spectrum of the solution taken at -70 °C was essentially unchanged, except for a downfield shift

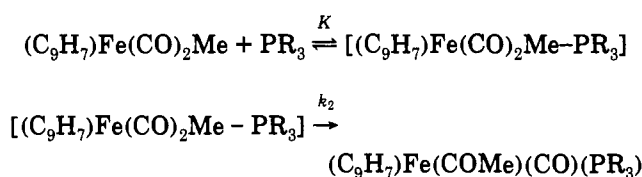
(23) Connors, K. A. *Binding Constants. The Measurement of Molecular Complex Stability*; Wiley-Interscience: New York, 1987; p 147.

(24) Beck, M. T. *Chemistry of Complex Equilibria*; Van Nostrand Reinhold: London, 1970; p 86.

of the same protons by 12–14 Hz, which was temperature dependent, as checked by a blank experiment on a solution of **1** alone. The shift observed at 0 °C increases with increasing concentration of PPh₃, whereas the methyl protons (δ -0.30) are virtually unaffected. In the ³¹P{¹H} NMR spectrum of PPh₃ (0.33 M) in toluene-*d*₈, the chemical shift of phosphorus moves downfield by only 3.4 Hz in the presence of complex **1** (0.14 M), whereas that of the product (C₉H₇)Fe(CO)(COMe)(PPh₃) is 79.0 ppm downfield from PPh₃.

Discussion

In the analysis of reaction rates as a function of a reactant, deviations from linearity often provide the most revealing information about the mechanism. This is the case for the reaction of complex **1** with the phosphines PMe₂Ph, PMePh₂, and PPh₃, as shown in Figures 2 and 3. The tendency toward saturation is typical of a reaction proceeding through formation of kinetically detectable intermediates.^{12,21,25} The increasing rate difference with increasing concentration of phosphine among different phosphines represents a guiding criterion toward the formulation of the mechanism in terms of Scheme II, adapted as follows to our system:



The phosphine, as part of a molecular complex [(C₉H₇)Fe(CO)₂Me–phosphine], formed in rapid preequilibrium, activates carbon–carbon coupling and affects the rate of the alkyl migration step. The observed reaction is a combination of the two-step sequence, and the *k*₂*K* products (Table III) represent a meaningful comparison of reactivity throughout the series under subsaturating conditions.

The Molecular Complex [(C₉H₇)Fe(CO)₂Me–PR₃]. The methyl complex (C₉H₇)Fe(CO)₂Me and phosphine interact rapidly, with respect to the migratory insertion process, and generate an equilibrium with a new species of 1:1 stoichiometry. The independent observation of the species [(C₉H₇)Fe(CO)₂Me–PPh₃] by UV–visible spectroscopy and the agreement of the quantitative analysis for the determination of the equilibrium constant *K* with the values obtained from rate data give full support to the mechanism proposed.

The FTIR and ¹H NMR spectra obtained at high phosphine concentration, in order to bias the equilibrium toward the molecular complex [(C₉H₇)Fe(CO)₂Me–PPh₃], give no indication of significant structural variations with respect to the indenyl complex alone. In the range 0.4–1.0 M PPh₃, the relative amount of the molecular complex and of (C₉H₇)Fe(CO)₂Me varies between 1.5 and 3. The ¹H NMR spectrum of [(η³-C₉H₇)Fe(CO)₃[–](PPh₃)₂N⁺] exhibits large shifts (1–2 ppm), upfield for the C_{1,3}H doublet and downfield for the C₂H triplet, with respect to η⁵ structures,⁴⁸ whereas we observe only small downfield shifts for (C₉H₇)Fe(CO)₂Me in the presence of PPh₃. The shifts of the carbonyl IR stretching bands to lower frequencies (~1 cm⁻¹) and of the C_{1–3}H protons to lower field (~1.5 Hz), although difficult to disentangle from trivial medium effects, along with the increase of the molar absorptivity of **1** in the presence of PPh₃ are all in the sense of altered electron density in the metal complex. The experiments seem to indicate the existence of a weak interaction between phosphine and (C₉H₇)Fe(CO)₂Me which does not perturb the molecular frame of the iron complex. This is

typical of loose complexes of *closed-shell* electronic structures, in which the identities of the original molecules are largely preserved.²⁶

The kinetics of the migratory insertion reaction offers the opportunity to evaluate the interaction of the methyl complex with the different phosphines. The equilibrium constants *K* show little variation with the nature of the phosphine but clearly indicate that association increases from PMe₂Ph to PPh₃. It is possible that the increasing stability of the molecular complex upon replacement of methyl by phenyl groups in PR₃ depends on enhanced π-acceptor ability of the phosphine.^{26,27} The increasing stability of the species [(C₉H₇)Fe(CO)₂Me–PR₃] is also reflected in reduced reactivity of the migratory insertion process, as indicated by the values of *k*₂ (Table III). In fact, the reaction of **1** with the trialkylphosphine PMe₃ produces a simple second-order kinetic pattern, in agreement with the presence of the highly reactive species [(C₉H₇)Fe(CO)₂Me–PMe₃], probably formed as an unstable encounter complex.²³

At this stage of the present work, we would consider it an over simplification to discuss further the binding forces responsible for the molecular association between the complex (C₉H₇)Fe(CO)₂Me and the phosphines. Certainly, the phenomenon is in agreement with the recognized ability of indenyl complexes to interact with incoming ligands. However, ring slippage of the indenyl group toward a species of the type [(η³-C₉H₇)Fe(COMe)(CO)(PR₃)], at this stage of the reaction, is not supported by the experiments. This is in agreement with the fact that indenyl η³ species have been postulated as intermediates or transition states formed in the rate-determining step.^{1,2,7,48,9}

Because of the peculiarity of the phenomenon observed and the potential relevance in organometallic reactivity, our experiments address the importance of further investigation in order to explore the properties and the roles of the molecular complexes here detected. Spectroscopic evidence has been recently presented that coordinatively saturated organometallic molecules are capable of forming unstable adducts with small molecules.²⁸

In principle, the kinetic analysis cannot distinguish between the mechanism described in Scheme II and the formation of an unreactive molecular complex on the side of the reaction coordinate.²³ For instance, such an interaction may be that of the phosphine facing the upper side of the indenyl ligand, opposite the reaction center. However, this interaction may be expected to be quite general, independent of the type of reaction occurring at the metal center, and previous evidence should then have appeared from the consistent body of kinetic work in substitution reactions on indenyl complexes.^{1,2,10}

The Alkyl Migration Step (*k*₂). The carbon–carbon coupling occurs in a slow monomolecular process within the species [(C₉H₇)Fe(CO)₂Me–phosphine]. The rate constants *k*₂ increase with increasing basicity and decreasing cone angle of the phosphine,²⁹ which represents further evidence of nucleophilic activation in the migratory insertion reaction.^{13,14,16e,30} The rate constant *k*₂ varies more with temperature than does the equilibrium constant *K*. The effect of the temperature has been studied with PPh₃, between 40 and 60 °C, lower and higher temperatures not being suited to the kinetic experiments. The activation parameters for the alkyl migration step are Δ*H*[‡] = 18.8 ± 1 kcal mol⁻¹ and Δ*S*[‡] = -20.1 ± 3 cal K⁻¹ mol⁻¹. In agreement with a reaction occurring within a binary complex, the activation entropy is less negative than the values observed in typical bimolecular reactions of indenyl complexes, which usually run between -30 and -40 cal K⁻¹ mol⁻¹.^{11,9}

(26) Mulliken, R. S.; Person, W. P. *Molecular Complexes*; New York, Wiley-Interscience: New York, 1969.

(27) (a) Orpen, A. G.; Connelly, N. J. *Organometallics* **1990**, *9*, 1206. (b) Orpen, A. G. *J. Chem. Soc., Dalton Trans.* **1991**, 653.

(28) Lokshin, B. V.; Greenwald, I. I. *J. Mol. Struct.* **1990**, *222*, 11.

(29) Tolman, C. A. *Chem. Rev.* **1977**, *77*, 313.

(30) Bellachioma, G.; Cardaci, G.; Macchioni, A.; Reichenbach, G. J. *Organomet. Chem.* **1992**, *427*, C37.

(25) Atwood, J. D. *Inorganic and Organometallic Reaction Mechanisms*; Brooks/Cole Publishing Company: Monterey, CA, 1985; p 15.

The transformation of the complex $[(C_9H_7)Fe(CO)_2Me\text{-phosphine}]$ into the product involves both iron-phosphorus bond formation and alkyl migration, which may occur either simultaneously or in sequence. A sequence of steps may imply the formation of an $[(\eta^3-C_9H_7)Fe(CO)_2Me(\text{phosphine})]$ structure, which could either form as a rapidly reacting intermediate or as a transition state. However, both of these conditions prevent the possibility of direct observation, and the existence of an η^3 species along the reaction coordinate still remains a speculative subject. In alternative, alkyl migration assisted by attack of phosphorus at metal would not imply ring slippage. This picture is in agreement with the conclusions of a kinetic study of migratory insertion in $(C_5H_5)Mo(CO)_3Me$, described in terms of direct attack of nucleophilic tetrahydrofuran at the metal center while methyl migration occurs.^{14a} Rate enhancements by nucleophiles were predicted by the results of a MO study of methyl migration in pentacarbonylmethylmanganese(I), in which a concerted process was envisioned.^{14b} In the oxidatively promoted carbonylation of $(C_5H_5)Fe(CO)(L)(Me)$, the transition state of the rate-determining step has been proposed as formally heptacoordinate by incorporation of a solvent molecule and electron-rich compared to the ground state.^{16c}

The methyl complex $(C_5H_5)Fe(CO)_2Me$ only reacts with triphenylphosphine in polar solvents and at high temperatures³¹ and proved to be inert during carbonylation.^{8a} We have observed

some reactivity with PMe_2Ph and $PMePh_2$ in the direction of eq 2 in toluene but were unable to obtain meaningful kinetic data. This confirms the higher reactivity of the indenyl complex, but a meaningful comparison between indenyl and cyclopentadienyl, in terms of reactivity and mechanism, cannot be obtained with the methyl complexes.

Conclusions

This work presents clean kinetic evidence that the migratory insertion reaction of the 18-electron indenyl dicarbonyl methyl complex $(C_9H_7)Fe(CO)_2Me$ is nucleophilically induced by the incoming phosphine. The experiments rule out the formation of solvent-saturated or 16-electron acyl intermediates, typical of migratory insertion reactions, and do not give evidence of $(\eta^3\text{-indenyl})M$ intermediates. Kinetic and spectroscopic data are in agreement with the rapid and reversible formation of a weak complex between the phosphine and the indenyl iron complex, followed by rate-determining rearrangement within the inner sphere of the metal involving alkyl migration and complete iron-phosphorus bond formation.

Acknowledgment. A travel award from NATO is gratefully acknowledged (Collaborative Research Grant 900289).

(31) Bibler, J. P.; Wojcicki, A. *Inorg. Chem.* **1966**, *5*, 889.